Secondary electron emission near the electronic stopping power maximum

R. Neugebauer, R. Wuensch, T. Jalowy, and K. O. Groeneveld
Institut für Kernphysik der Johann-Wolfgang-Goethe-Universität, August-Euler-Strasse 6, Frankfurt am Main, Germany

H. Rothard
Centre Interdisciplinaire de Recherches Ions-Laser (CEA-CNRS-ISMRA), Rue Claude Bloch, Boîte Postale 5133, 14070 Caen Cedex 05, France

A. Clouvas
Department of Electrical and Computer Engineering, Aristotle University of Thessaloniki, GR-54006 Thessaloniki, Greece

C. Potiriadis
Greek Atomic Energy Commission, GR-15310 Agia Paraskevi, Greece
(Received 20 October 1998; revised manuscript received 22 January 1999)

We report on measurements of light ion ($Z=2$) and heavy ion ($Z=14$) induced electron emission yields from the entrance and exit surfaces of thin carbon foils near the electronic energy loss per unit path length (dE/dx) maximum. At constant dE/dx, secondary electron yields are lower for high projectile velocities than for lower projectile velocities. This velocity effect, which is well known for secondary ion emission, is observed for backward electron emission for both He and Si. In the case of Si projectiles such a velocity effect is also observed for forward electron emission. The results can be qualitatively understood in the framework of recent electron transport and nuclear track models. [S0163-1829(99)08617-8]

INTRODUCTION

The interaction of fast charged particles with a condensed matter leads to secondary particle emission. Electrons, atoms, and molecules (neutral or ionized) are ejected from the entrance and exit surfaces of solids if sufficiently thin foils are used. The knowledge of the mean number of electrons emitted per incoming projectile (the electron yield γ) gives important information about basic interaction mechanisms between ion and solid. Important applications concern track formation in solids, detectors of heavy ions, and tumor treatment by heavy ion beams, just to name a few. Extensive reviews on electron emission from solids can be found in Refs. 1–3.

Electron yields were found to be proportional to the electronic energy loss per unit path length dE/dx for proton impact on carbon for both exit and entrance surface as function of projectile velocity over a wide range of velocities.[4] For heavy ions, the ratio $\Lambda=\gamma/(dE/dx)$ was found to increase with the projectile velocity above the stopping-power maximum.[5] It should be interesting to correlate the electron yields and dE/dx in the projectile velocity region around the dE/dx maximum where the same dE/dx value may occur at two different projectile velocities v_p. In the present work the correlation between electron yields and energy loss was studied around the dE/dx maximum with helium and silicon projectiles.

EXPERIMENT

The experimental work was performed at the 2.5 MV Van De Graaff accelerator of the Institut für Kernphysik in Frankfurt am Main for the helium projectiles and at the 5 MV Tandem accelerator of the National Research Center of Physical Sciences ''Demokritos'' in Athens in Greece for the silicon projectiles. Mass analyzed beams of He^{+}, He^{++} (0.2–2 MeV), and Si^{6+} (12–27 MeV) were sent through thin (500 Å) self-supporting carbon foils. The thickness of the targets was large enough to ensure that (i) the charge equilibrium of the penetrating particles was reached before the ions reached the exit surface and (ii) full development of the secondary electron cascade induced by high-energy δ electrons was achieved. The experiments were performed under high vacuum conditions ($p<10^{-4}$ Pa).

The experimental setup used in Athens is the same as in Ref. 4. The experimental setup used in Frankfurt is almost identical and has been described in detail in Ref. 6. Two nearly closed metal cylinders (similar to Faraday cages, except for openings for the incoming and outgoing ion beam) mounted on each side of a target-foil holder were used to collect the secondary electrons in forward and backward directions of the target foil simultaneously, but separately. The cylinders were held at a positive potential $+U_0=+40$ V to assure that all the secondary electrons were collected, and a negative potential of $-U_0=-20$ V was applied to the target, enough for the electron emission yield to reach a saturation value. The Faraday cup was comprised of two parts: a beam-collecting cup that was grounded through an electrometer and a cylindrical electrode upstream of this cup which was biased $-U_{\mathrm{rep}}=-300$ V with respect to the ground. This negatively biased electrode prevented (i) secondary electrons from escaping from the collecting cup and (ii) secondary electrons of the target from escaping through the opening of the outgoing ion beam of the second cylinder, the so-called γ cup. A similar repeller was positioned upstream of the first γ cup and biased $-U_{\mathrm{rep}}=-300$ V with respect to the ground

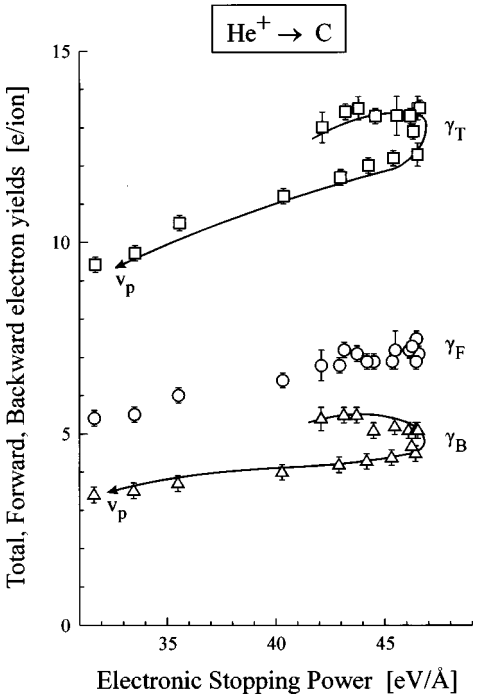

FIG. 1. The dE/dx dependence of γ_B, γ_F, γ_T for incident He^+ ions. The lines guide the eye, the arrows point to increasing v_p.

in order to prevent (i) secondary electrons from the slits to hit the first γ cup and (ii) secondary electrons of the target from escaping through the opening of the incoming ion beam of the first γ cup.

Backward (γ_B), forward (γ_F), and total (γ_T) electron yields can easily be deduced from measuring: the ion induced target current I_T, the current in the two γ cups I_F and I_B, and the current in the Faraday cup I_{FC}:

$$\gamma_B = q_f\left(\frac{I_B}{I_{FC}}\right), \tag{1}$$

$$\gamma_F = q_f\left(\frac{I_F}{I_{FC}}\right), \tag{2}$$

$$\gamma_T = q_f\left(\frac{I_T}{I_{FC}}\right) + q_f - q_i, \tag{3}$$

where q_f is the mean final charge state of the projectiles after leaving the foil exit surface, and q_i is the projectile incident charge before the foil entrance. The mean charge q_f of the projectiles emerging from the carbon foils was obtained from Refs. 7–9.

RESULTS AND DISCUSSION

Figure 1 shows the electron yields γ_B, γ_F, γ_T obtained with He^+ projectiles of energies between 0.2–2 MeV as a function of the electronic energy loss per unit path length (dE/dx). The electronic stopping power (dE/dx) values for He in carbon were calculated with the TRIM code.[10] The lines through the data points guide the eye, the arrows indicate increasing v_p direction. At constant (dE/dx) both γ_B and γ_T are lower for high v_p than for low v_p. There is a clear velocity effect on γ_B and γ_T. Within error bars, however, no velocity effect on γ_F can be seen.

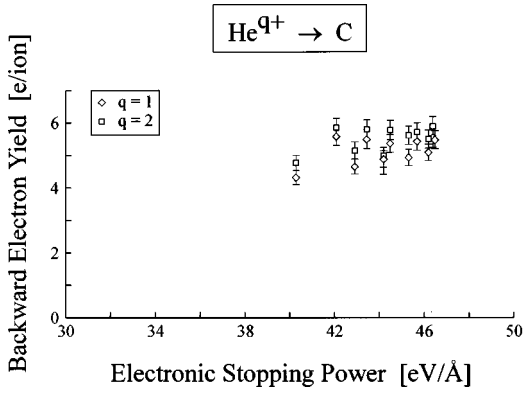

FIG. 2. The dE/dx dependence of γ_B for incident He^{++} and He^+ ions.

In the phenomenological model on electron emission based on the Sternglass treatment,[11–12] kinetic emission of electrons is considered as a three-step process: (1) production of the secondary electrons near the entrance and exit surface of the foil; (2) transport of secondary electrons towards the entrance and exit surface of the foil; (3) escape of the secondary electrons from the target surfaces. It is now well established[12] that ''nonequilibrium near surface stopping powers'' are correlated to the production of the secondary electrons both at the entrance and exit surface of the foil. These pre-equilibrium stopping powers are reduced in comparison to the calculated TRIM bulk energy-loss values. At constant (dE/dx) value the production of electrons in the entrance surface of the foil at the corresponding high and low velocities may in addition be different due to the role of the projectile electron of He^+. The projectile electron while it is bound to the nucleus screens the nuclear charge therefore reducing the stopping power. Nevertheless, if it is lost and acts as independent particle, it can produce additional secondary electrons (passive and active role, see Ref. 4). Since the production of the secondary electrons varies with the square of the partly screened nuclear charge, it is reasonable to assume that even for helium ions the contribution of the projectile electron in the backward emission is small compared to the contribution due to the nuclear charge. The screening of the nuclear charge by the projectile electron of He^+ varies as function of the penetration depth. Since most of the emitted electrons originate from within a depth much smaller than the depth needed to reach charge equilibrium, one can expect a higher screening for high projectile velocity than for low velocity. The low charge state remains ''frozen'' in the thin surface layer of about 30 Å (Ref. 13) from which most low-energy electrons originate. This leads to less production of secondary electrons for high velocity than at low velocity, in agreement with the experimental observations. In order to test the above mentioned hypothesis, we measured the backward electron emission induced by He^+ and He^{++} ions for the same projectile velocity. As can be seen from Fig. 2, a reduced backward electron emission for He^+ ions compared to the backward emission induced by He^{++} projectiles is observed for all projectile velocities. This can be attributed to the screening of the nuclear charge by the projectile electron. The velocity effect observed in Fig. 2 for both He^+ and He^{++} ions, however, indicates that further

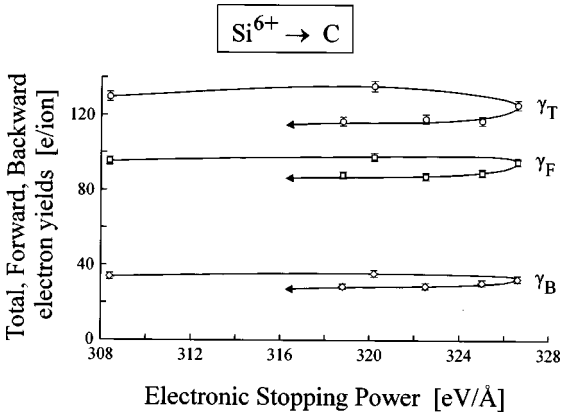

FIG. 3. The dE/dx dependence of γ_B, γ_F, γ_T for incident Si^{6+} ions. The lines guide the eye, the arrows point to increasing v_p.

different mechanisms must be responsible for the experimental observations.

A simple explanation which can describe qualitatively the experimental observations obtained with He^+ and He^{++} ions is the following. During the passage of the incident ions through the carbon foil target atoms are ionized, the electrons (both low energy electrons from soft collisions at large impact parameter and high energy (δ) electrons from violent, binary, close collisions) move away from their ''place of birth.'' If the solid surface is within the range of these electrons and if they have enough energy to overcome the surface potential barrier, they eventually leave the target. The δ electrons transport energy far away, and if they stay in the target bulk they dissipate the energy in cascading processes and production of more electrons of low energy (cascade multiplication). The transport of δ electrons is strongly peaked in forward direction.[5] The energy is partially transported away from the projectile entrance surface into the direction of the projectile exit surface. Thus at the projectile entrance surface at constant dE/dx, fewer secondary electrons are produced for high v_p than for low v_p. Similarly, γ_B is reduced for high v_p. At the projectile exit surface δ electrons transport energy into the vacuum. If the target is thick enough (target thickness larger than the range of δ electrons) the lost energy is replaced by δ electrons originating from the bulk. Therefore on the projectile exit surface we do not expect and do not observe a v_p dependence of γ_F.

This is not the case for Si^{6+} incident ions where a velocity effect is clearly observed also for the forward yield (Fig. 3). The above-mentioned electron transport model fails to describe the presence of a velocity effect for γ_F observed for silicon ions. On the contrary, a track model[14–16] can describe qualitatively the observed velocity effect in forward and backward electron emission. In the framework of a track model, the projectile deposits energy in a cylindrical volume (amorphous material) along the trajectory called ''infratrack'' or ''track core.'' [14] For some femtoseconds the core is a zone of highly charged, plasmalike target material (depending on the electrical conductivity). Energy is dissipated by δ-electron emission in a bulk area around the trajectory. This area is called the ''ultratrack'' or ''track halo.'' [14] δ electrons dissipate the energy in cascading processes into low-energy electrons. The dimension of this halo is given by the δ electrons range. Due to binary collisions, the δ electrons range increases with v_p and thus the dimension of the track halo. For the same amount of deposited energy per unit path length, i.e., for constant dE/dx, the energy density in the track depends on v_p. In the track model the secondary particle emission depends on the energy density in the surface regions of the track[15–16] and thus on v_p. Within this track picture, with increasing projectile velocity, the relative number of fast electrons is enhanced. A relative reduction of low-energy electron emission and possibly plasmon excitation for a given dE/dx occurs. The electron energy distribution is shifted towards higher energies, but the relative number of low-energy electrons (which dominates the yields) is lowered. This can easily explain the observed velocity effect not only in backward, but also in forward direction.

CONCLUSION

The correlation between electron yields and energy loss for helium and silicon projectiles around the dE/dx maximum was investigated. At constant dE/dx, secondary electron yields are lower for high projectile velocities than for lower projectile velocities. This effect was not observed for the forward electron emission obtained with helium ions. The ''velocity effect'' presented here can be qualitatively understood in the framework of electron transport and track models. A similar but larger effect is not only known[17] for the secondary ion emission, but it has also been found that the induced damage in solids[18] may depend on projectile velocity. In the studied projectile energy range, nuclear energy loss is negligible. Damage production in the solid and secondary ion emission from the surface can only be due to an electronic process. Therefore the electron transport in the solid is involved in the damage creation process. Both the ejected secondary ions and electrons are a probe for this process.

ACKNOWLEDGMENTS

This work was supported by GSI, Darmstadt. A.C. acknowledges financial support from the DAAD, Bonn. H.R. acknowledges support from the ''Service Culturel et Scientifique'' of the French Embassy in Greece.

[1] J. Devooght, J. C. Dehaes, A. Dubus, M. Cailler, J. P. Ganachaud, M. Rosler, and M. Brauer, in *Particle Induced Electron Emission I*, edited by G. Hohler and E. A. Niekisch, Springer Tracts in Modern Physics Vol. 122 (Springer-Verlag, Berlin, 1991).

[2] D. Hasselkamp, H. Rothard, K. O. Groeneveld, J. Kemmler, P. Varga, and H. Winter, in *Particle Induced Electron Emission II*, edited by G. Hohler and E. A. Niekisch, Springer Tracts in Modern Physics Vol. 123 (Springer-Verlag, Berlin, 1991).

[3] H. Rothard, Scanning Microsc. **9**, 1 (1995).

[4] A. Clouvas, C. Potiriadis, H. Rothard, D. Hofmann, R. Wuensch, K. O. Groeneveld, A. Katsanos, and A. C. Xenoulis, Phys. Rev. B **55**, 12 086 (1997).

[5] H. Rothard, M. Jung, M. Caron, J. P. Grandin, B. Gervais, A. Billebaud, A. Clouvas, and R. Wuensch, Phys. Rev. A **57**, 3660 (1998).
[6] H. Rothard, K. Kroneberger, E. Veje, A. Clouvas, J. Kemmler, P. Koschar, N. Keller, S. Lencinas, P. Lorenzen, O. Heil, D. Hofmann, and K. O. Groeneveld, Phys. Rev. B **41**, 3959 (1990).
[7] J. B. Marion and F. C. Young, *Nuclear Reaction Analysis, Graphs and Tables* (North-Holland, Amsterdam, 1968).
[8] A. Clouvas, M. J. Gaillard, A. G. Pinho, J. C. Poizat, and J. Remillieux, Nucl. Instrum. Methods Phys. Res. B **2**, 273 (1984).
[9] K. Shima, N. Kuno, M. Yamanouchi, and H. Tawara, At. Data Nucl. Data Tables **51**, 173 (1992).
[10] J. F. Ziegler and J. P. Biersack, in *The Stopping and Ranges of Ions in Solids* (Pergamon, New York, 1985).
[11] E. J. Sternglass, Phys. Rev. **108**, 1 (1957).
[12] P. Koschar, K. Kroneberger, A. Clouvas, M. Burkhard, W. Meckbach, O. Heil, J. Kemmler, H. Rothard, and K. O. Groeneveld, Phys. Rev. A **40**, 3632 (1989).
[13] M. Jung, H. Rothard, B. Gervais, J. P. Grandin, A. Clouvas, and R. Wuensch, Phys. Rev. A **54**, 4153 (1996).
[14] W. Brand and R. H. Ritchie, in *Physical Mechanisms in Radiation Biology*, edited by R. D. Cooper and R. D. Woods (USEC Technical Inf. Center, Oak Ridge, TN, 1974).
[15] B. U. R. Sundqvist, Int. J. Mass Spectrom. Ion Processes **126**, 1 (1993).
[16] P. K. Hakanson, Mat. Fys. Medd. K. Dan. Vidensk. Selsk. **43**, 593 (1993).
[17] R. Neugebauer, R. Wuensch, T. Jalowy, M. Kuzel, D. Hofmann, and K. O. Groeneveld, Nucl. Instrum. Methods Phys. Res. B **124**, 418 (1997).
[18] Z. G. Wang, C. Dufour, E. Paumier, and M. Toulemonde, J. Phys.: Condens. Matter **6**, 6733 (1994); **7**, 2525 (1995).